https://doi.org/10.1093/plphys/kiac464 PLANT PHYSIOLOGY 2023: 191: 610–625

Plant Physiology®

Research Article

Transition to ripening in tomato requires hormone-controlled genetic reprogramming initiated in gel tissue

Ximena Chirinos [1,2], Shiyu Ying,[1,2,3] Maria Aurineide Rodrigues [1,2,4], Elie Maza [1,2], Anis Djari [1,2], Guojian Hu [1,2], Mingchun Liu [3], Eduardo Purgatto [5], Sylvie Fournier,[6,7] Farid Regad [1,2], Mondher Bouzayen [1,2] and Julien Pirrello [1,2]*

1 Laboratoire de Recherche en Sciences Végétales—Génomique et Biotechnologie des Fruits—UMR5546, Université de Toulouse, CNRS, UPS, Toulouse-INP, Toulouse, France
2 Université de Toulouse, INRAe/INP Toulouse, Génomique et Biotechnologie des Fruits—UMR990, Castanet-Tolosan, France
3 Key Laboratory of Bio-Resource and Eco-Environment of Ministry of Education, College of Life Sciences, Sichuan University, Chengdu, Sichuan 610065, China
4 Institute of Biosciences, Department of Botany, Universidade de São Paulo, São Paulo, 11461 Brazil
5 Departamento de Alimentos e Nutrição Experimental, Faculdade de Ciências Farmacêuticas, Universidade de São Paulo, São Paulo, SP, Brazil
6 Metatoul-AgromiX platform, LRSV, Université de Toulouse, CNRS, UPS, Toulouse INP, France
7 MetaboHUB-MetaToul, National Infrastructure of Metabolomics and Fluxomics, Toulouse, 31077, France

*Author for correspondence: julien.pirrello@toulouse-inp.fr (J.P.)
These authors contributed equally (X.C., S.Y.).
J.P. and M.B. planned and designed the research. X.C., S.Y., M.A.R., and E.P. performed experiments. S.F. performed metabolomics experiments and data analysis. X.C., S.Y., A.D., and E.M. contributed to computational analysis. X.C., S.Y., G.H., M.L., F.R., J.P., and M.B. analyzed data. X.C., J.P., and M.B. wrote the manuscript.
The author responsible for distribution of materials integral to the findings presented in this article in accordance with the policy described in the Instructions for Authors (https://academic.oup.com/plphys/pages/general-instructions) is: Julien Pirrello (julien.pirrello@toulouse-inp.fr).

Abstract

Ripening is the last stage of the developmental program in fleshy fruits. During this phase, fruits become edible and acquire their unique sensory qualities and post-harvest potential. Although our knowledge of the mechanisms that regulate fruit ripening has improved considerably over the past decades, the processes that trigger the transition to ripening remain poorly deciphered. While transcriptomic profiling of tomato (*Solanum lycopersicum* L.) fruit ripening to date has mainly focused on the changes occurring in pericarp tissues between the Mature Green and Breaker stages, our study addresses the changes between the Early Mature Green and Late Mature Green stages in the gel and pericarp separately. The data showed that the shift from an inability to initiate ripening to the capacity to undergo full ripening requires extensive transcriptomic reprogramming that takes place first in the locular tissues before extending to the pericarp. Genome-wide transcriptomic profiling revealed the wide diversity of transcription factor (TF) families engaged in the global reprogramming of gene expression and identified those specifically regulated at the Mature Green stage in the gel but not in the pericarp, thereby providing potential targets toward deciphering the initial factors and events that trigger the transition to ripening. The study also uncovered an extensive reformed homeostasis for most plant hormones, highlighting the multihormonal control of ripening initiation. Our data unveil the antagonistic roles of ethylene and auxin during the onset of ripening and show that auxin treatment delays fruit ripening via impairing the expression of genes required for System-2 autocatalytic ethylene production that is essential for climacteric ripening. This study unveils the detailed features of the transcriptomic reprogramming associated with the transition to ripening of tomato fruit and shows that the first changes occur in the

Received June 30, 2022. Accepted September 16, 2022. Advance access publication October 6, 2022

locular gel before extending to pericarp and that a reformed auxin homeostasis is essential for the ripening to proceed.

Introduction

Fruit ripening is the last phase of fleshy fruit development that ultimately leads to fruit decay and seed dispersal. During this process, most fruit quality traits occur as a result of the activation of major physiological and metabolic pathways, leading to changes in color, aroma, and texture. These traits are essential in making the fruit attractive to consumers and frugivores that promote seed dispersal. It is commonly accepted that ripening starts at the breaker stage when the fruit color shifts from green to light yellow. Based on their ripening profiles, fruits are classified as climacteric or nonclimacteric depending on whether or not they undergo a rise in respiration and in autocatalytic ethylene production (Klee and Giovannoni, 2011). A typical characteristic of climacteric fruit is their capacity to initiate ripening when detached from the plant, once they gain the competence to ripen, a stage commonly named Mature Green (MG). Ethylene has been considered the primary hormone orchestrating climacteric fruit ripening. Consequently, a plethora of studies have been devoted to the role of this hormone in the ripening process (Lelièvre et al., 1997; Liu et al., 2015). Also, it is worth mentioning that, so far, most studies have focused on deciphering the dynamic changes taking place in the pericarp tissues while neglecting what occurs in inner tissues.

The ethylene biosynthetic pathway involves two specific steps catalyzed by 1-aminocyclopropane-1-carboxylate (ACC) synthase (ACS) and ACC oxidase (ACO), both encoded by multigene families. In climacteric fruit like tomato (*Solanum lycopersicum* L.), at the pre-ripening immature green stages, ethylene biosynthesis is controlled by the so-called System-1 characterized by auto-inhibitory ethylene production, whereas System-2 prevails at MG stages and is characterized by autocatalytic ethylene production (Lelièvre et al., 1997; Giovannoni et al., 2017). System-1 ethylene production mainly relies on ACS1A, ACS6, and ACO1, while System-2 is dependent on ACO1, ACO4, ACS2, and ACS4 (Oeller et al., 1991; Nakatsuka et al., 1998; Barry et al., 2000; Liu et al., 2015). The transition from System-1 to System-2 ethylene biosynthesis marks the beginning of the climacteric phase and acquisition of ripening competency (McMurchie et al., 1972). How ethylene production shifts from auto-inhibitory to auto-catalytic during the transition to ripening is still unclear.

It is remarkable that potential roles of other hormones during the transition to ripening of climacteric fruit remains poorly understood. Several studies have reported that exogenous applications of auxin (indole-3-acetic acid, IAA), gibberellic acid (GA), or cytokinin (CK) delay ripening (Dostal and Leopold, 1967; Davey and Van Staden, 1978; Su et al., 2015). On the other hand, exogenous applications of abscisic acid (ABA), brassinosteroid (BR), or jasmonate (JA) have been reported to promote ripening and enhance climacteric ethylene production (Zhang et al., 2009; Zhu et al., 2015; Tao et al., 2021). Although these studies support the hypothesis that these hormones may have important roles in fruit ripening, there is little understanding of their possible interactions with ethylene. It was recently shown that auxin, ABA, and JA influence the expression of genes involved in the ripening control network, including those involved in ethylene biosynthesis (Li et al., 2021). In addition, a growing body of evidence supports the importance of crosstalk between different hormones in controlling tomato fruit ripening. It was demonstrated that *ETHYLENE RESPONSE FACTOR B3* (*SlERF.B3*), encoding a TF from the Ethylene Response Factor (ERF) family, is responsive to both ethylene and auxin and integrates these two signaling pathways via regulation of the auxin signaling component *SlIAA27* (Liu et al., 2018). Moreover, the expression of the auxin conjugating gene *GRETCHEN HAGEN 3* (*GH3*) is upregulated by ABA and ethylene during grape (*Vitis vinifera*) and tomato ripening, suggesting the existence of complex multihormonal crosstalk associated with the process of fleshy fruit ripening (Böttcher et al., 2011; SravanKumar et al., 2018). ABA has been reported to induce ripening by promoting ethylene biosynthesis in banana (*Musa sapientum* L.), tomato, and peach (*Prunus persica laevis* L. Batsch) (Zhang et al., 2009; Soto et al., 2013; Jiang et al., 2014) in line with enhanced transcript levels of *ACS2*, *ACS4*, and *ACO1* genes upon exogenous ABA application (Chernys and Zeevaart, 2000; Zhang et al., 2009).

Overall, our knowledge of the molecular mechanisms and factors underlying the shift from ripening incompetency to ripening competency associated with the transition to ripening is sparse. We recently proposed a model in which RIPENING INHIBITOR (SlRIN) and SMALL AUXIN UPREGULATED 69 (SlSAUR69) define a regulation loop that acts as a modulator of the balance between auxin and ethylene via repressing auxin transport and tissue distribution, resulting in enhanced ethylene sensitivity (Shin et al., 2019). However, a more comprehensive understanding of the molecular events controlling the developmental transition leading to the initiation of the ripening process is still missing.

The development of high-throughput sequencing technologies has paved the way for transcriptomic profiling aimed at deciphering the dynamic changes in gene expression on a genome-wide scale. This effort has greatly benefited from the characterization of ripening-impaired mutants, including *ripening inhibitor* (*rin*) and *non-ripening* (*nor*) (Kumar et al., 2018). Both mutants produce dominant-negative TFs capable of repressing many key ripening-related genes (Ito et al.,

2017; Wang et al., 2019; Li et al., 2020). Knockout or knockdown lines have demonstrated that *RIN* and *NOR* are required for the full progression of ripening (Ito et al., 2017; Wang et al., 2019; Li et al., 2020). Several other MADS-box TFs essential for the expression of multiple ripening genes, including *TOMATO AGAMOUS-LIKE1 (TAGL1)* and *FRUITFULL (FUL1* and *FUL2*), form DNA-binding complexes with MADS-RIN (Itkin et al., 2009; Bemer et al., 2012; Fujisawa et al., 2014). Among the NAC TFs, *NOR-like1*, *NAC4*, and *NAC9* positively regulate ethylene biosynthesis and lycopene production (Gao et al., 2018; Kou et al., 2018). Re-evaluation of the regulatory hierarchy of key ripening regulators has been made with the recent insights provided by clustered regularly interspaced short palindromic repeats/Cas9 (CRISPR/Cas9) technology (Wang et al., 2019; Li et al., 2021), but data exploring their role in hormone biosynthesis and signaling genes during the ripening process are scarce.

In tomato, the ripening process has been addressed by focusing mainly on the pericarp tissue, likely due to the fact that the onset and progression of ripening are typically associated with visible changes in the external color of the pericarp. However, although fruit texture and softening are associated with the ripening phase, it was recently demonstrated that this major fruit quality trait is dependent on differentiation of the locular tissue and determined at early pre-ripening stages (Huang et al., 2021). This finding represents a paradigm shift in thinking and clearly points out the important role of tissues besides pericarp in controlling the ripening process. Previous studies have indicated that initial ripening steps, including pigment accumulation and locular differentiation, take place within the fruit inner tissues (Shinozaki et al., 2018). Furthermore, the rise in the expression of many important ripening-associated genes like *RIN*, *NOR*, *PECTIN-LYASE1 (PL1)*, *PHYTOENE SYNTHASE1* (*PSY1*), and *CAROTENOID ISOMERASE* (*CRTISO*) begins in the locular tissue and then radiates out to the placenta and other tissues. Altogether, these data call for more attention to the investigation of physiological and transcriptomic regulation in the gel and pericarp tissues separately. In the present study, we present genome-wide transcriptomic profiling of the transition to ripening in tomato pericarp and gel, spanning four ripening stages. Notably, while most studies exploring the transition to ripening considered the transcriptomic changes in the whole fruit, a distinctive feature of our study is to sample separately the gel and pericarp in order to reveal potential differences and shifted dynamics of the transcriptomic reprogramming associated with the transition to ripening in the two tissues. Moreover, whereas the MG stage is commonly considered as a homogeneous stage, and in an attempt to capture the very early events heralding the transition to ripening, our study distinguishes Early Mature Green (EMG) and Late Mature Green (LMG) as two different development stages. The data reveal that the transcriptomic reprogramming associated with initiation of ripening occurs first in the gel tissue before extending to the pericarp. The transcriptomic analysis also comprehensively identified TF families contributing to the transcriptomic reprogramming underlying the ripening initiation and provided several potential candidate TFs putatively involved in the transition to ripening. In addition, the study documents changes in multiple hormone signaling pathways, indicating that fruit ripening is under complex multihormonal control. Finally, the study uncovered a key role for auxin and its interplay with ethylene during the onset of ripening.

Results

Transcriptomic changes associated with the transition to ripening are initiated in the locular gel tissue

To unravel the transcriptomic reprogramming associated with the transition to ripening, we performed whole-genome transcriptomic profiling by RNA sequencing (RNA-Seq) of tomato fruit at four developmental stages, including EMG, LMG, Breaker (Br), and 4-day post-breaker (Br + 4). Moreover, to investigate whether ripening initiation is synchronized in all parts of the fruit organ, we sampled the pericarp and locular gel tissues separately. On average, 44 million clean reads were generated per sample and mapped to the SlyMIC v.1.0 assembly and annotation of the *S. lycopersicum cv.* MicroTom reference genome (BioProject: PRJNA553986). The total number of differentially expressed genes (DEGs) during the transition to ripening was 18,134 genes in gel tissue and 16,863 in the pericarp (Figure 1A). Principal component analysis (PCA) revealed major differences between the transcriptomes generated, with 57% of the variance (PC1) associated with the ripening stages and 24% of the variance (PC2) with the tissue type. The gel transcriptome gives rise to clusters distinct from those of the pericarp at both ripening (Br and Br + 4) and pre-ripening (EMG and LMG) stages. Notably, the two pericarp transcriptomes corresponding to the pre-ripening stages cluster together, while these EMG and LMG stages cluster separately in the gel, with the LMG gel transcriptome starting to shift toward that of the ripening stages. This clustering suggests that the transition to ripening starts earlier in the gel than in pericarp tissue, as shown by the higher extent of transcriptomic changes revealed during the transition from EMG to LMG in the gel tissue (Figure 1B). Consistent with this idea, the number of DEGs between EMG and LMG is more than twice higher in the gel (829) than in the pericarp (318; Figure 1A). However, throughout the progression toward ripening, the number of DEGs between LMG and Br becomes similar in the gel (11,867) and pericarp (9,515), and this trend continues when considering the DEGs between Br and Br + 4 (5,210 in pericarp and 5,601 in the gel). As a complementary nontargeted approach, we examined co-expressed gene sets reflecting tissue or stage specificity, using weighted gene co-expression network analysis (WGCNA). A total of 21 modules were identified based on the similar expression patterns (Supplemental Figure S1, A and B) highlighting the existence of tissue or stage-specific modules. In particular, M7 and M8

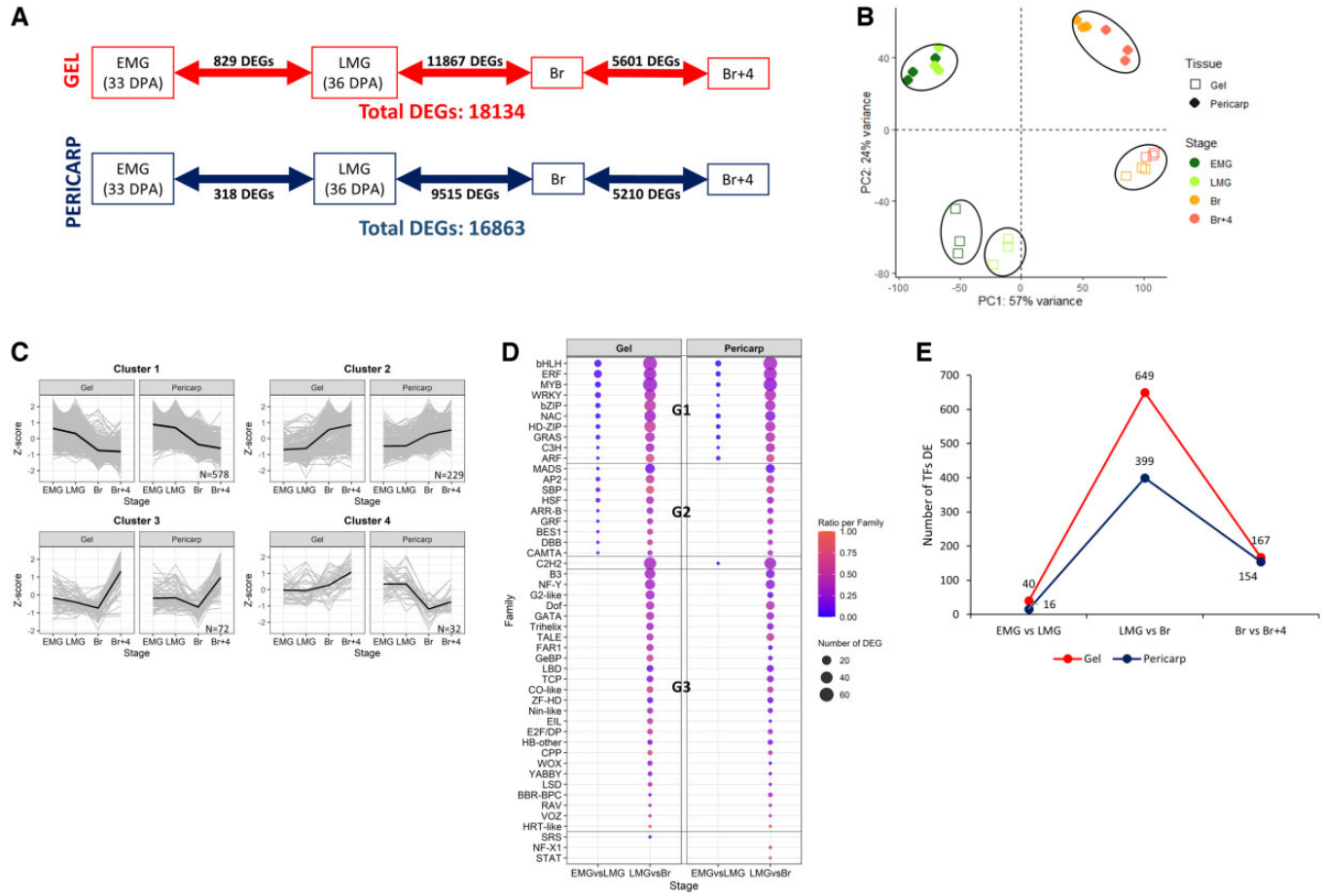

Figure 1 Global transcriptomic changes during the transition to ripening in tomato fruit. A, Transcriptional dynamics throughout ripening showing the number of DEGs at early stages of the transition to ripening. B, PCA of transcriptomic profiles of EMG, LMG, Br, and Br + 4 in gel and pericarp tissues. Every symbol represents one replicate. C, Clustering analysis of DEGs corresponding to TFs at four ripening stages in gel and pericarp according to their expression pattern. The bold black line represents the mean *z*-score for each cluster. D, Dot-plot showing the number of TF family members that are DEGs when comparing pre-ripening and early-ripening stages. The dot color indicates the ratio between the number of DEGs per family/total number of family members in the tomato genome. E, The number of TFs displaying differential expression during ripening in gel and pericarp. Adjusted $P < 0.05$.

modules gather genes whose expression is highly correlated with the gel tissue while the expression of genes in M18, M19, and M3 modules is strongly correlated with pericarp. On the other hand, the expression of genes in modules M1, M4, and M13 is highly correlated with the developmental stages.

Because any transcriptomic reprogramming requires the intervention of TFs, we sought to capture all DEGs annotated as putative TFs. Among a total of 1,994 TF genes in the tomato genome, 911 exhibit differential expression (DE) during the transition to ripening in the pericarp and gel tissues. The clustering of DEG TFs based on their expression pattern during ripening revealed four main clusters (Figure 1C). Cluster 1 includes 578 genes that show downregulation at the transition from LMG to Br in both gel and pericarp. Cluster 2 contains 229 TF genes that are upregulated during the initiation of ripening, including several known ripening regulators (*RIN*, *NOR*, *FUL2*, *CNR*, *TAGL1*, *NAC4*, *AP2A*, and *SlARF2A*). In particular, *RIN*, *NOR*, and *AP2a* show substantial increases in their transcript levels between EMG and LMG in locular gel tissues and only moderate upregulation in the pericarp (Supplemental Figure S2). In contrast, the upregulation of *FUL1* in the pericarp precedes that in the gel. Cluster 3 includes 72 genes that are upregulated once ripening has been initiated. Finally, Cluster 4 includes 32 genes showing opposite trends, upregulated in the gel, while downregulated in the pericarp. Taken together, the data support the idea that transcriptomic reprogramming associated with ripening initiation follows shifted dynamics in the gel and pericarp.

The high number and enormous diversity of TF families involved in the transition to ripening in tomato fruit reflect the extent of transcriptomic reprogramming underlying this process (Figure 1C; Supplemental Table S1). Indeed, out of 54 TF families identified in the tomato genome, 48 showed at least one differentially expressed member during ripening initiation (Figure 1D). Three main groups of TF families were defined based on their expression profiles. Group 1 (G1)

contains 10 TF families whose members show DE between the four ripening stages in both gel and pericarp. Of these, basic helix–loop–helix (bHLH), ERF, NAC, and MYB TF families are the most representative of G1 and contain more members potentially engaged in these transitions. The second group (G2) contains TF families whose members display DE only in locular gel between the pre-ripening stages EMG and LMG, with APETALA2 (AP2), SQUAMOSA promoter Binding Protein-like (SBP), HEAT SHOCK FACTOR (HSF), and MADS-Box being the most represented families in this group. The third group (G3) includes TF families specifically differentially expressed between LMG and Br. Given that Group 2 members are differentially expressed specifically in the gel at the pre-ripening stages and become DEGs in the pericarp only later at the transition from LMG to Br, they are good candidates for active regulators orchestrating the initiation of ripening. In line with the idea that transcriptomic reprogramming is more intensive in the gel than in the pericarp at ripening initiation, 40 genes encoding putative TFs are differentially expressed between the EMG and LMG stages in the gel but only 16 in the pericarp (Figure 1E). At the transition from LMG to Br, 649 TF genes are DEGs in the gel and 399 in the pericarp. Finally, the number of TF genes that exhibit a statistically significant change in their expression level between Br and Br + 4 becomes similar in the gel (167) and the pericarp (154). The dynamics and changes that occur in TF genes reflect the extent of the global transcriptomic reprogramming and support the idea that the pericarp undergoes similar changes to those occurring in the gel but with a time lag. Notably, the comprehensive analysis of TF genes during the transition to ripening defines potential candidates putatively involved in the regulation of the transcriptional network associated with the initiation of the ripening process in tomato fruit (Supplemental Table S1).

The transcriptomic reprogramming underlying the transition to ripening is associated with multiple hormone-associated processes

To further define the biological processes associated with fruit ripening, we performed a GO term enrichment analysis of all DEGs in gel and pericarp separately. The analysis indicated that, among the top 20 most enriched GO terms, the GO:0009755 corresponding to hormone-mediated signaling pathway was highly enriched in both tissues (Supplemental Figure S3A). To gain better insight into the hormonal control of the transition to ripening in tomato fruit, we identified all DEGs related to hormone signaling, metabolism, and transport. Remarkably, genes associated with almost all plant hormones are affected at the transition to ripening, including auxin, ethylene, ABA, JA, BR, SA, CK, and GA, ordered based on the number of DEGs (Supplemental Figure S3B). Strikingly, while ethylene is known to be the primary hormone regulating climacteric fruit ripening, transcriptomic profiling revealed that auxin-related processes exhibit the highest number of DEGs (Supplemental Figure S3B). The data indicate that several genes related to the biosynthesis and signaling of CK, GA, and auxin are downregulated (Supplemental Figure S4, A–C). On the other hand, JA, ABA, and BR biosynthesis and signaling genes are upregulated, while the expression of genes involved in the catabolism of these hormones is decreased (Supplemental Figure S4, D–F). Hormone profiling showed that the levels of the CK active form dihydrozeatin decrease during the onset of ripening (Supplemental Figure S5A). This finding is consistent with the downregulation of CK-biosynthesis genes and the previously reported negative role of CKs during ripening (Davey and Van Staden, 1978). On the other hand, ABA and the glucose-conjugated form ABA–glucose ester levels increased at the initiation of ripening, in line with the transcriptomic profile of their related genes (Supplemental Figures 4, E and 5, B). Surprisingly, JA levels decrease at the Br stage, likely due to the transformation of JA into JA-Ile active form by *GRETCHEN HAGEN 3* (*GH3*) *JASMONATE RESISTANT* (*JAR*) genes (Supplemental Figures 4, D and 5, C). Overall, the data clearly indicate that the transition to ripening involves alterations in processes associated with multiple hormones.

Based on the number of the corresponding DEGs between EMG and LMG, auxin, ethylene, BR, and JA appear to be the most involved in the events initiating the ripening program (Figure 2A). Later, at the transition from LMG to Br stage, the highest number of DEGs occurs with auxin and ethylene processes, suggesting that the interplay between these two hormones may have a prominent role at the onset of ripening (Figure 2A). Clustering analysis of auxin-related DEGs at early stages of ripening identified two groups, one includes 81 genes that show downregulation as the main trend during ripening initiation and the second includes 31 genes exhibiting upregulation during later ripening stages (Figure 2B). Interestingly, Cluster 1 contains 23 genes involved in auxin biosynthesis, including one *TRYPTOPHAN AMINOTRANSFERASE* (*TAA*), and two *FLAVIN-CONTAINING MONOOXYGENASES* (*YUC*) genes (Figure 2C). On the other hand, Cluster 2 contains several *SMALL AUXIN UP-REGULATED* (*SAUR*) genes including *Sl-SAUR69* that is greatly upregulated at Br stage and shown to negatively regulate auxin transport (Shin et al., 2019; (Figure 2, B and D); two *GRETCHEN HAGEN 3* (*GH3*) IAA–amido synthetases, including *SlGH3-2*, an ortholog of grape *GH3.1* that preferentially conjugates aspartate to IAA (Böttcher et al., 2011; SravanKumar et al., 2018); and one *DIOXYGENASE FOR AUXIN OXIDATION* (*DAO*) encoding a DAO enzyme that irreversibly oxidizes IAA or IAA-Asp (Hayashi et al., 2021; Figure 2C). Together, these results are consistent with a pattern in which the expression of genes associated with auxin synthesis decrease, whereas those associated with auxin catabolism increase during the transition from LMG to Br. Consistent with the outcome of this interpretation of transcriptomic profiling, levels of active forms of free auxin decrease, while conjugated inactive forms accumulate in the fruit tissue at the onset of ripening (Figure 2E). Altogether,

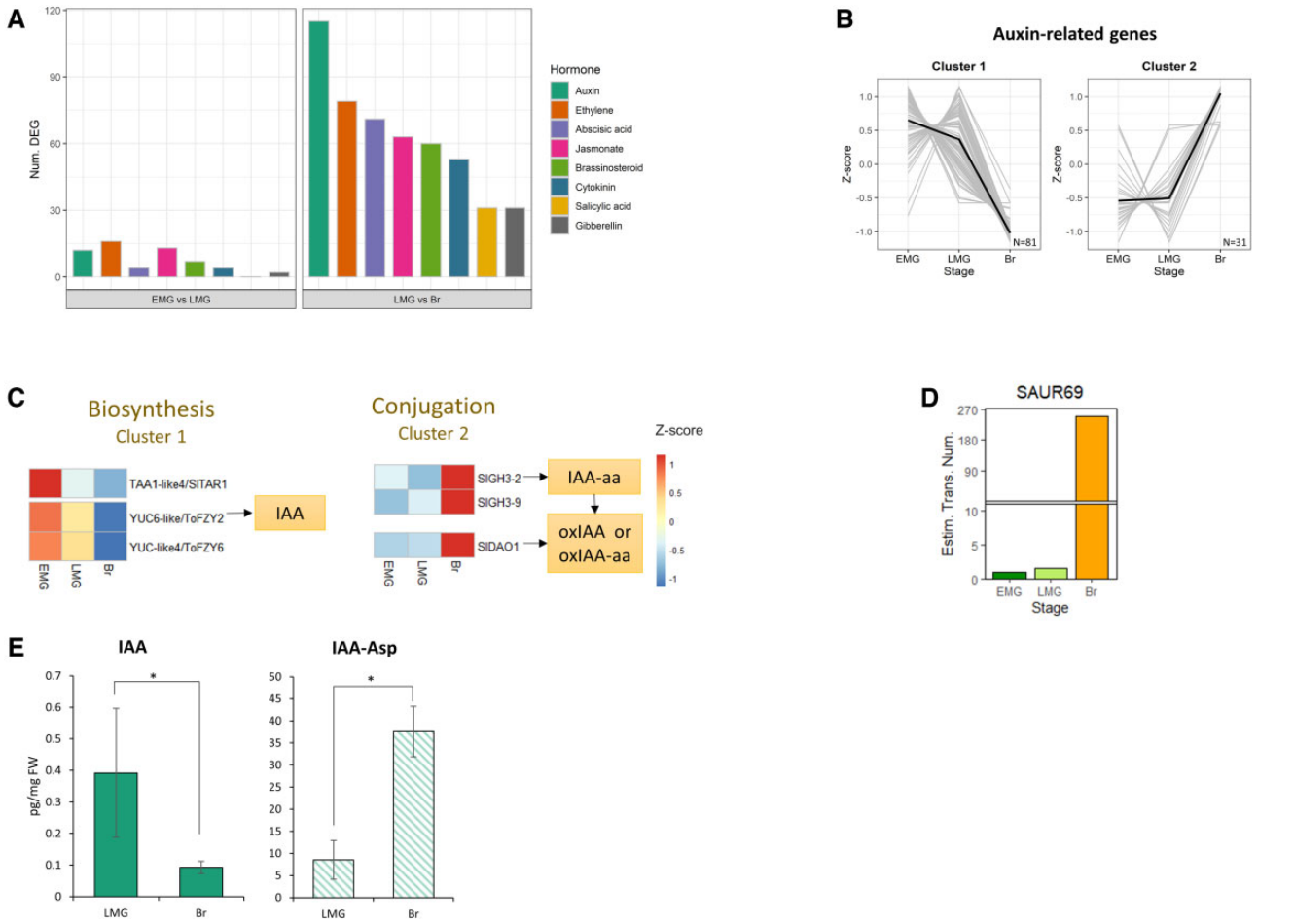

Figure 2 Hormone-associated DEGs during the transition to ripening. A, Number of DEGs related to each hormone at two transition stages EMG versus LMG and LMG versus Br (adjusted $P < 0.05$). B, Cluster analysis of auxin-related DEGs at pre-ripening stages. C, Heatmap the expression level of genes involved in auxin biosynthesis (IPA pathway) and conjugation. D, Estimated transcript number of *SlSAUR69* at pre-ripening stages. E, Endogenous levels of free IAA and its conjugated form IAA–Asp at the initiation of ripening. Results shown are mean ± SE, based on three independent biological replicates. Statistical significance was determined using Student's *t* test: $^*P < 0.05$.

the data suggest that a fundamental shift in auxin metabolism occurs at the onset of ripening, likely through cross-talk with ethylene, as reported previously (Hao et al., 2015; Liu et al., 2018; Shin et al., 2019).

Auxin treatment delays the transition to ripening

Considering the high number of DEGs related to auxin during the transition to ripening, we set out to further explore the role of this hormone in ripening initiation by performing two successive treatments with exogenous auxin (IAA, 100 μM) at 33 DPA (EMG) and 34 DPA (Figure 3A). Because transcriptomic profiling showed that similar changes in the overall gene expression occur in the gel and the pericarp, albeit with some delay in the latter tissue, we decided to address the impact of auxin treatment on the whole fruit. In contrast to the mock-treated fruit that undergo typical ripening as indicated by the color change, the auxin-treated fruit exhibited delayed and incomplete change in color until 12 days after treatment (Figure 3B). This is consistent with the previous reports indicating that auxin acts as a negative regulator of fruit ripening (Su et al., 2015; Li et al., 2016, 2017; Tobaruela et al., 2021). To further decipher the changes induced by auxin treatment during the initiation of ripening, we performed genome-wide transcriptomic profiling on fruit samples collected at three time points. The first transcriptome was from fruit sampled 6 h after the first injection and addressed potential wound effect of the treatment as well as early auxin responses. The second and third transcriptomes correspond to fruit sampled 24 h and 72 h after the second injection, respectively (Figure 3A).

PCA indicated that 6-h and 24-h transcriptome data cluster together, suggesting that these two time points are representative of short-term responses to exogenous auxin treatment and probably responses to mechanical wounding due to the injections (Figure 3C). In contrast, transcriptomes corresponding to 6-h and 24-h samples are separated from the 72-h samples which likely represent long-term responses to auxin. Consistent with this hypothesis, the total numbers of DEGs between auxin-treated and mock samples were 14,038 DEGs and 13,140 after 6 h and 24 h, respectively, and

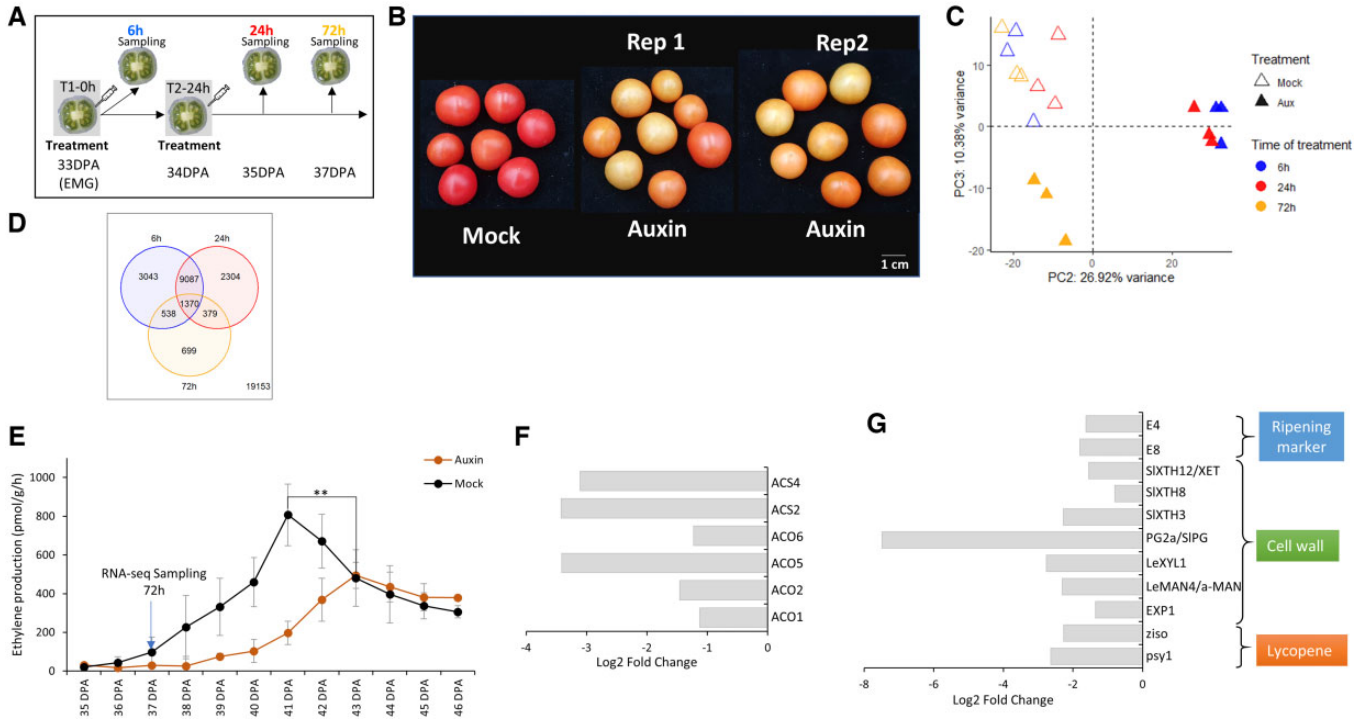

Figure 3 Impact of exogenous auxin treatment on tomato fruit ripening. A, Experimental design of the study. Tomato fruits were injected at 33 DPA (T1) with mock or auxin and the treatment was repeated after 24 h (T2). Samples were collected at three time points: 6 h after T1, 24 h after T2, and 48 h after T2. B, Ripening phenotype at 45 DPA (12 days after T1) of mock and auxin-treated fruits. The pictures are representative of at least 10 independent replicates showing the same trend. Among these independent replicates, three were used for the transcriptomic profiling by RNA-Seq. Images were digitally extracted for comparison. C, PCA of transcriptomic profiles of mock or auxin-treated fruits at 6 h after T1, 24 h, and 72 h after T2. Each symbol represents one replicate. D, Venn diagrams of the number of DEGs (auxin vs. mock) at 6 h after T1, 24 h, and 72 h after T2. E, Ethylene production in tomato fruits treated with mock (black line) or auxin (orange line) (mean ± SD, $n = 10$, based on three independent biological replicates). F, G, Bar plot representing log2(fold change) values of DEGs at 72 h after treatment, auxin vs. mock (adjusted $P < 0.05$) for ethylene biosynthesis genes (F) and ripening-associated genes (G). T1, first treatment; T2, second treatment. Asterisks indicate significant differences determined by Student's *t* test at $^{**}P < 0.01$.

thereafter dropped to 2,986 at 72 h. Most of the DEGs, either up- or downregulated, are shared between the 6-h and 24-h samples (Figure 3D), revealing that auxin treatment induces massive transcriptomic changes early after the injection. Thereafter, the transcriptomic landscape stabilized at 72 h after treatment. We therefore postulated that the 72-h transcriptome data, rather than the 6 h or 24 h ones, reflect a sustainable auxin effect on ripening. This result prompted us to focus our study on the 72-h samples to uncover the genes and networks altered by auxin during the onset of ripening.

To assess the potential effect of auxin treatment on ripening, we first monitored ethylene production in mock- and auxin-treated fruits. The rise in ethylene production is delayed in auxin-treated fruits, which also produced less ethylene than mock-treated fruit (Figure 3E), supporting the hypothesis that auxin negatively controls ethylene production during climacteric fruit ripening. Consistent with this interpretation, transcript levels of the ethylene biosynthesis genes *ACS2*, *ACS4*, *ACO1*, *ACO2*, *ACO5*, and *ACO6*, known to be involved in System-2 ethylene production, were all downregulated 72 h after auxin treatment (Figure 3F).

In order to address whether the reduced ethylene production in IAA-treated tomatoes is due to their inability to induce autocatalytic System-2, we treated the fruit with propylene, an ethylene analog known to mimic the hormone effects. Propylene treatment restored normal ripening and ethylene production in auxin-treated fruits. Notably, both mock- and auxin-treated fruit challenged with 100 ppm propylene leads to almost a complete recovery of ethylene production, indicating that auxin treatment does not hamper the activation of System-2 but rather impairs ethylene biosynthesis (Supplemental Figure 6, A and B). In line with the reduced ethylene production, the expression of *E4* and *E8*, well-known ethylene-responsive and ripening-regulated genes, was also downregulated. Moreover, many important, well-characterized ripening-associated pathways were altered by auxin. For instance, the carotenoid biosynthesis genes *PSY1* and *ZISO* are downregulated in auxin-treated fruits, consistent with the faint red pigmentation in these fruits (Figure 3G). Likewise, the expression of cell wall-related genes, including *EXPANSIN 1* (*EXP1*), *a-MAN*, *LeXYL1*, *POLYGALACTURONASE 2a* (*PG2a*), *SlXTH3*, *SlXTH8*, and *XET*, is reduced in auxin-treated fruit (Figure 3G). Together, these data indicate that auxin treatment alters multiple ripening-

associated pathways through impairing ethylene biosynthesis.

Auxin alters the expression of TF genes encoding key regulators of fruit ripening

To further decipher how auxin alters the transcriptomic reprogramming underlying the transition to ripening, we analyzed the impact of auxin treatment on the expression of TF genes. A total of 174 TF genes belonging to 35 different TF families are differentially expressed in auxin-treated fruit. Among these, 14 families exhibited members undergoing either up- or downregulation, 10 families exhibited only downregulation, and 11 families exhibited only upregulation (Figure 4A). Consistent with auxin being a negative regulator of ripening, TF genes encoding key regulators of tomato fruit ripening, including *RIN*, *NOR*, *AP2a*, *NAC1*, and *FUL1*, were all downregulated in auxin-treated samples (Figure 4B).

Because the ERF family had the highest number of downregulated genes upon auxin treatment, and considering the important role ascribed to ERFs in mediating ethylene responses, we analyzed their expression patterns during ripening initiation. Notably, among the 77 *ERF* genes present in the tomato genome, 42 (68%) showed a statistically significant change in their transcript levels during the transition to ripening, and based on the expression profiles, two ERF clusters were identified; one cluster includes 13 genes upregulated at the onset of ripening, and the second cluster includes 39 genes that are downregulated (Figure 4C). Interestingly, six out of the nine *ERF* genes that are upregulated during ripening initiation in untreated fruit are downregulated by auxin treatment, including *SlERF.E1* and *SlERF.E4*, both known to be highly induced at the onset of ripening (Figure 4C). On the other hand, among the 33 *ERF* genes that are downregulated during ripening initiation, 12 are differentially regulated by auxin, among which five show upregulation (Figure 4C). The data reveal the strong impact of auxin on the expression of several *ERF* genes, which may reflect altered ethylene responses following auxin application. The data are consistent with previous reports showing that, in addition to their response to ethylene, *ERF* genes can also be regulated by auxin (Pirrello et al., 2012).

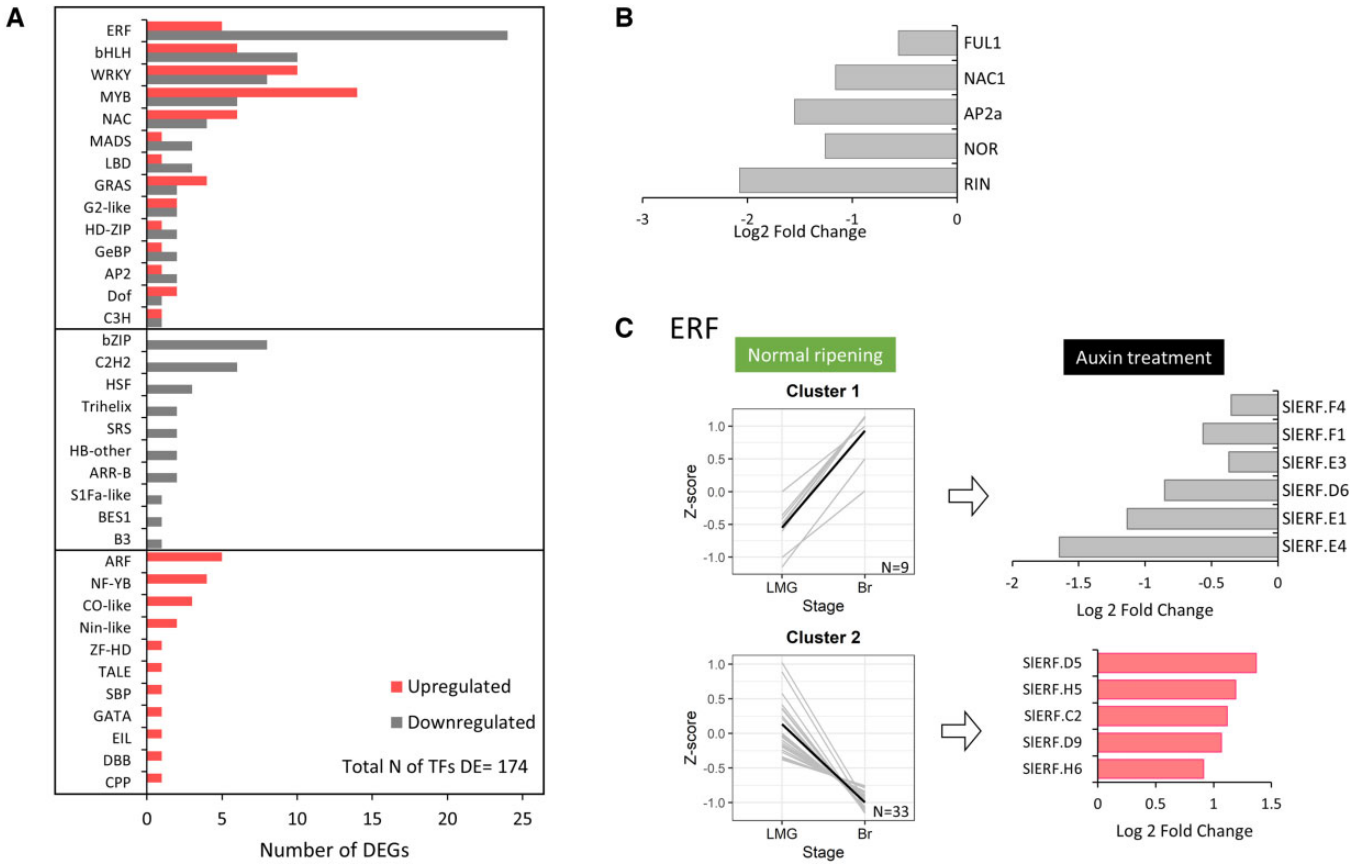

Figure 4 Impact of auxin treatment on the expression of transcription factor genes that are DEGs. A, Number of TF genes being DEGs 72 h after auxin treatment in each family. Downregulated genes are shown in grey (log2(fold change) < 0, adjusted $P < 0.05$), and upregulated genes in red (log2(fold change) > 0, adjusted $P < 0.05$). B, Expression of key ripening regulator TFs after 72 h of auxin treatment. C, Clustering of *ERF* genes being DEGs at the onset of ripening in normal ripening fruit (left). Bar plot representing log2(fold change) values of the expression level of ERF after auxin treatment (right).

Auxin treatment alters hormonal signaling during ripening

The transcriptomic profiling indicated that the transition to ripening is associated with modulation of several hormones (Figure 2A). Strikingly, among the 673 hormone-related DEGs during ripening (Supplemental Figure S3B; Supplemental Table S2), 113 exhibited DE following auxin treatment (Supplemental Table S2). Under normal ripening, genes related to ethylene are distributed in two clusters. Cluster 1 contains 29 genes that are upregulated at the onset of ripening, 17 of which are downregulated in response to auxin treatment (Figure 5A). Interestingly, these genes whose expression is modulated by auxin are involved in all steps of ethylene signaling, including biosynthesis (*ACS2*, *ACS4*, *ACO1*, *ACO2*), signal transduction (*ETR3*, *ETR6*, *EBF2*, *EBF3*), and transcriptional activation (*SlERFE.E1*, *SlERF.E4*). Cluster 2 includes 48 genes that are downregulated at the transition to ripening, including five ERFs (*SlERF.C2*, *SlERF.D5*, *SlERF.D9*, *SlERF.H5*, and *SlERF.H6*). The copper transporter *RAN1* genes exhibit upregulation upon auxin treatment (Figures 4, C and 5,A). These data indicate that auxin treatment greatly disturbs the expression of many ethylene-associated genes, including those involved in System-2 ethylene production, likely causing the observed delayed ripening. This observation is consistent with the requirement for a decline in auxin signaling essential for initiation of climacteric ripening (Shin et al., 2019).

Abscisic acid has been reported to influence fruit ripening in different ways, depending on the mode and timing of application (Diretto et al., 2020). Cluster analysis shows that 20 ABA-related genes are upregulated (Cluster 1) during normal ripening and four of these genes are downregulated by auxin treatment, including *SlCYP707A3*, an ABA 8′-hydroxylases involved in ABA oxidative catabolism, as well as the putative ABA response genes *HVA22K-like* and *HVA22K-like1* (Figure 5B). Cluster 2 includes 41 genes downregulated during ripening, and among these, auxin treatment remarkably upregulates *MOCOS-like2* and *AAO4-like5* 2 genes

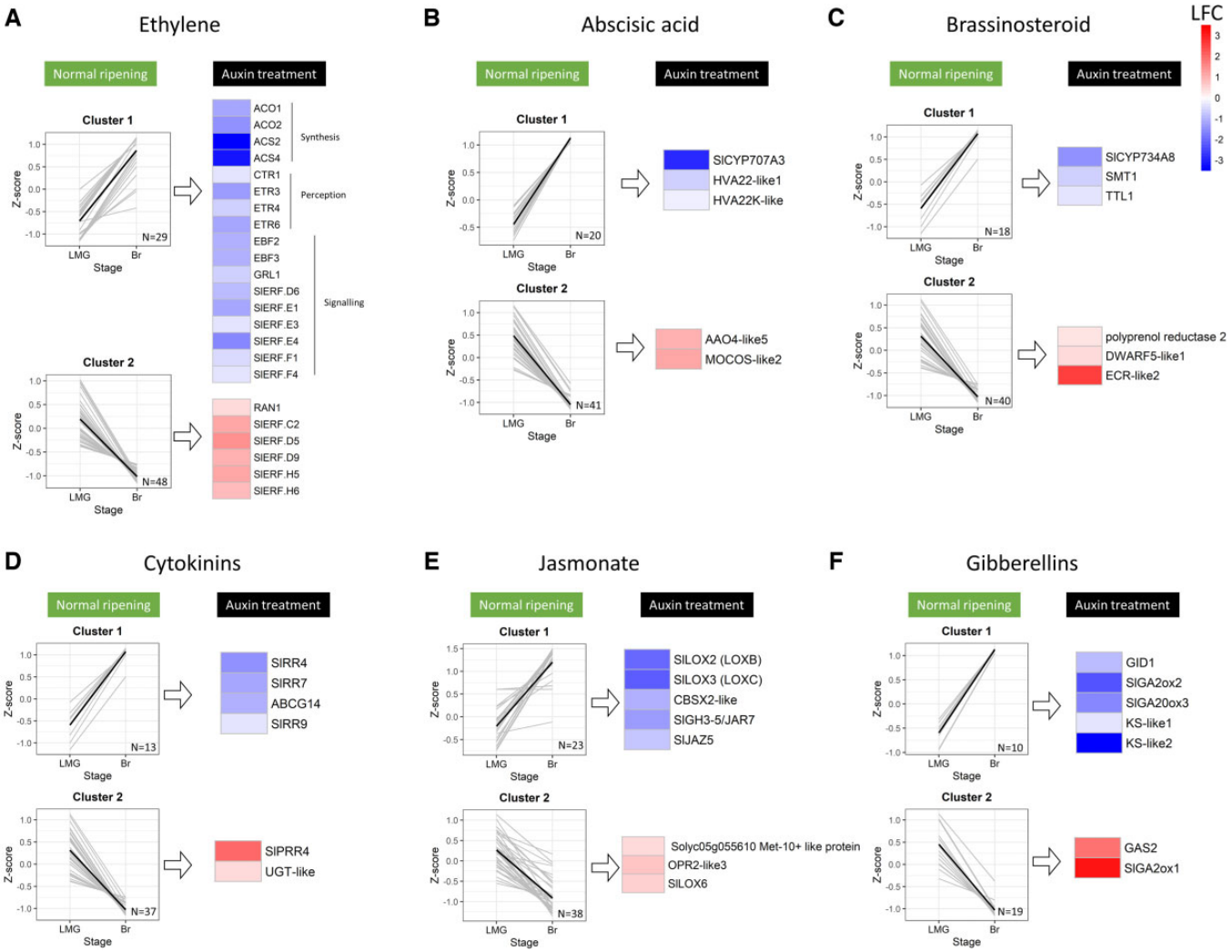

Figure 5 Impact of auxin treatment on the expression of hormone-related genes. Clustering of hormone-related genes in normal ripening (left) or auxin-treated (right). Right shows genes displaying opposite trend upon auxin treatment (72 h). A, Ethylene, (B) abscisic acid, (C) brassinosteroid, (D) cytokinins, (E) jasmonate, and (F) gibberellins. Square color per gene represents log2(fold change). *N*, number of genes. Adjusted $P < 0.05$.

involved in ABA biosynthesis (Figure 5B). These data indicate that the expression of ABA-related genes is disturbed by exogenous auxin treatment.

Several studies have reported on a positive role for BR in fruit ripening (Hu et al., 2020). Analysis of BR-related genes undergoing differential regulation at the transition to ripening showed that 18 genes are upregulated (Cluster 1), while 40 are downregulated (Cluster 2; Figure 5C). Auxin treatment resulted in downregulation of three genes in Cluster 1, including *SlCYP734A8*, a gene encoding an enzyme putatively involved in BR catabolism. Upon auxin treatment, three genes involved in BR biosynthesis belonging to Cluster 2 were upregulated (Figure 5C). These results support the hypothesis that auxin promotes BR biosynthesis.

Studies on the role of CK in ripening are scarce, although it has been reported that CK levels decrease during ripening (Davey and Van Staden, 1978). Cluster analysis of genes related to CK showed that 13 genes are upregulated (Cluster 1) and 37 are downregulated (Cluster 2) at the onset of ripening. Within Cluster 1, three genes were downregulated after auxin treatment, including *SlRR4* and *SlRR7*, two Type-ARABIDOPSIS RESPONSE REGULATORS (ARRs) known to be negative regulators of cytokinin signaling, as well as *ABCG14*, a putative transporter of CK. In Cluster 2, two genes were upregulated after auxin treatment, including the ARABIDOPSIS PSEUDO-RESPONSE REGULATORS *SlPRR4* gene, described as effectors of cytokinin signal (Figure 5D), suggesting that auxin may enhance cytokinin signaling during the transition to ripening.

Cluster analysis of genes related to JA revealed 23 upregulated (Cluster 1) and 38 downregulated (Cluster 2) genes during ripening. Among Cluster 1 genes, five were downregulated by auxin treatment, including the main lipoxygenases contributing to JA biosynthesis, as well as C5 and C6 flavor volatiles, *SlLOX2* and *SlLOX3* (Figure 5E). Interestingly, *SlLOX2*, also known as *TomLoxC*, is the main contributor to tomato aroma (Shen et al., 2014). This observation is consistent with the previously described negative role of auxin in desirable volatile production (Tobaruela et al., 2021). Importantly, *SlJAR7*, a GH3 involved in the transformation of JA to its active form JA-Ile, is also downregulated, suggesting a negative role of auxin in JA biosynthesis. Surprisingly within Cluster 2, three genes annotated as putatively involved in JA biosynthesis are upregulated after auxin treatment (Figure 5E).

Exogenous application of GA was reported to delay tomato ripening (Dostal and Leopold, 1967). We, therefore, examined the behavior of genes related to GAs during normal fruit ripening, showing that 10 genes are upregulated (Cluster 1), while 19 are downregulated (Cluster 2; Figure 5F). Within Cluster 1, five genes are downregulated upon auxin treatment, including those related to GA biosynthesis *ent*-kaurene synthase *KS-like1* and *KS-like2*, a gibberellin 20-oxidase (*GA20ox3*), and a gibberellin catabolism gene, gibberellin 2-oxidase 2 (*SlGA2ox2*). Within the Cluster 2 downregulated genes, two corresponding to 2-oxoglutarate-dependent dioxygenase (*GAS2*), encoding enzymes mediating the last step in biosynthesis of the bioactive form of GA, DHGA12, undergo upregulation after auxin treatment (Figure 5F).

Altogether, our data suggest that auxin is capable of altering the expression of genes involved in the biosynthesis, catabolism, or signaling of multiple hormones during the transition to the ripening of tomato fruit.

Discussion

Fruit ripening is initiated in the gel

Fruit ripening is a complex process regulated by internal signals such as hormones and external cues like light and temperature. The developmental transition associated with ripening relies on major transcriptomic reprogramming, leading to a large number of biochemical and physiological changes, including changes in color and texture. Our knowledge of the mechanisms regulating fruit ripening has substantially progressed over the last several decades, and recent reports indicated that key ripening transcription factors are induced first in the locular gel prior to the pericarp (Giovannoni et al., 2017; Shinozaki et al., 2018). Most studies addressing fruit ripening have focused on the characterization of events occurring in the pericarp while neglecting the changes in locule and placenta tissues, although few studies indicated that the first changes that herald the onset of ripening occur in the locular gel at the time this inner tissue undergoes liquefaction with an early increase in ACC synthase activity in the gel tissue (Brecht, 1987; Van de Poel et al., 2014). In the case of climacteric fruit, the onset of ripening is a key step marked by the acquisition of ripening competency. The high number and vast diversity of TF families engaged in the transition to ripening revealed by our study reflects the complexity of this developmental process. Our analysis of the TF genes throughout fruit ripening suggests spatiotemporal specialization of distinct family members, thereby defining putative biologically relevant regulatory genes. Transcriptomic profiling of the transition to ripening in tomato fruit performed in our study confirms that the key ripening regulators *RIN* and *NOR* are first induced in the gel tissue between EMG and LMG stages, indicating that fruit ripening is initiated in the locule compartment (Supplemental Figure S2). DE analysis identified over 900 TF genes belonging to 48 different families putatively involved in the transition to ripening, reflecting the complexity of this developmental process. Among these genes, 13 members of the *bHLH* gene family and 12 members of the *GRAS* family undergo significant changes in their transcript levels during the early stages of ripening (Figure 1D; Supplemental Table S1). This observation is in line with the reported downregulation of SlbHLH95 that affects accumulation of total carotenoids, lycopene, as well as ethylene sensitivity (Zhang et al., 2020). Likewise, silencing of *SlGRAS38* results in lower lycopene content and reduced ethylene

production in tomato fruit, while the overexpression of *SlGRAS4* leads to premature ripening (Liu et al., 2021). Moreover, among the group of TFs that show DE in locular gel tissue earlier than in pericarp, *SlAP2a* has been demonstrated to be a negative regulator of ripening initiation and ethylene production and a positive regulator of chlorophyll degradation and carotenoid biosynthesis (Chung et al., 2010; Karlova et al., 2011; Wang et al., 2019). Overall, the data provide targets for future studies aiming to further decipher the regulatory network underlying the ripening process in tomato fruit.

Transition to ripening is a multihormone-controlled process with a prominent role for the interaction between auxin and ethylene

Given the central role of ethylene in climacteric fruit ripening, a large number of studies have focused on the mode of action of this hormone, whereas comparatively, the roles of other hormones in this transition are less well understood (Grierson, 2014; Liu et al., 2015). Therefore, a major challenge is to gain a comprehensive understanding of the molecular circuits underlying fruit ripening and to uncover the network of interactions between various hormones. Our data support the requirement for a reprogramming of multiple plant hormones at the onset of ripening. Indeed, we observed significant alterations in the expression of genes associated with all of the hormones that we examined, including auxin, ethylene, ABA, BR, CK, SA, JA, and GA. Moreover, the transition to ripening in tomato fruit involves an active interplay between auxin and ethylene. This result is consistent with our previous work showing that ripening initiation is associated with decreased auxin signaling that results in increased ethylene sensitivity, in turn leading to stimulation of System-2 ethylene production triggering climacteric ripening (Shin et al., 2019; Li et al., 2021).

Interestingly, ethylene treatment of IAA-treated fruits restores full ripening (Supplemental Figure S6A), and System-2 ethylene production can be induced by propylene in IAA-treated fruits (Supplemental Figure S6B). The response to propylene is a classic test for the initiation of autocatalytic ethylene synthesis during climacteric ripening (McMurchie et al., 1972). The restored autocatalytic ethylene biosynthesis in IAA-treated fruits suggests that the induction of System-2 ethylene production is tightly regulated by an ethylene/IAA balance in the fruit tissues. These results support the hypothesis that the decrease of auxin content is required for climacteric process to proceed at the onset of ripening. It is known that free auxin levels are highly dependent on conjugation to sugars and amino acids and that this process is integral to auxin homeostasis. While a comprehensive and accurate quantification of auxin and its conjugates at the onset of ripening is still lacking, our data reveal a depletion of free auxin at the onset of ripening and a concomitant increase in conjugated IAA–Asp. The study also revealed upregulation of several *GH3* genes, supporting the hypothesis that modulation of auxin homeostasis is a key step during the transition to ripening. Moreover, our transcriptomic profiling revealed that *SlSAUR69* is highly expressed at the Br stage, supporting the idea that auxin transport and tissue distribution may also contribute to the control of auxin homeostasis. Indeed, SlSAUR69 has been described as a negative regulator of polar auxin transport, generating auxin minima that result in enhanced ethylene sensitivity (Shin et al., 2019).

High auxin levels seem to impair all ripening-associated processes. Indeed, fruits treated with IAA display delayed ripening resulting in fruit that fail to reach full red color (Figure 3B), consistent with the downregulation of carotenoid biosynthesis genes (Figure 3G). The impaired ripening is also associated with downregulation of genes encoding cell wall modifying enzymes. Auxin and ethylene cross-talk has been reported to operate in many physiological processes including fruit ripening. It was shown that 7 days after auxin treatment, the transcript levels of genes involved in System-1 ethylene production are enhanced, whereas a high methylation status of genes involved in System-2 ethylene biosynthesis is maintained, resulting in the repression of their expression (Li et al., 2016). Our study shows that auxin treatment also results in downregulation of the key ripening gene *RIN*, known to control the expression of several ripening-associated genes encoding ethylene biosynthesis enzymes such as *ACS2* and *ACS4*, the ethylene receptor *ETR3*, cell-wall softening enzymes *PG2a* and *EXP*, carotenoid synthesis enzymes *PSY* and *ZDS* as well as TFs like *NAC-NOR*, *CNR*, *AP2a*, and *FUL1/2* (Fujisawa et al., 2011). This pattern of regulation raises the hypothesis that auxin may act through RIN to control the expression of ripening-related genes, in agreement with the recently elaborated model, in which ethylene initiates ripening at the MG stage, which in turn induces *SlSAUR69*, involved in auxin depletion and enhanced ethylene sensitivity (Shin et al., 2019; Li et al., 2020). Our data support this model by showing that high auxin levels block System-2 genes, and that auxin conjugation is a major component involved in the regulation of auxin homeostasis during normal fruit ripening (Figure 6). Nevertheless, the ability of ethylene to trigger ethylene synthesis suggests that the shift from System-1 to System-2 ethylene production is not dependent on auxin only. Although based on our present data, it is not possible to make a solid assumption in this respect, a plausible hypothesis would be that high concentrations of ethylene are required to reverse the inhibitory effect of auxin, which implies that the inhibition of System-2 by auxin can only be alleviated when ethylene concentrations reach a certain threshold level. More experiments are needed to validate this hypothesis.

Overall, the study unravels in a renewed way the transcriptomic reprogramming associated with the transition to ripening of tomato fruit and highlights the

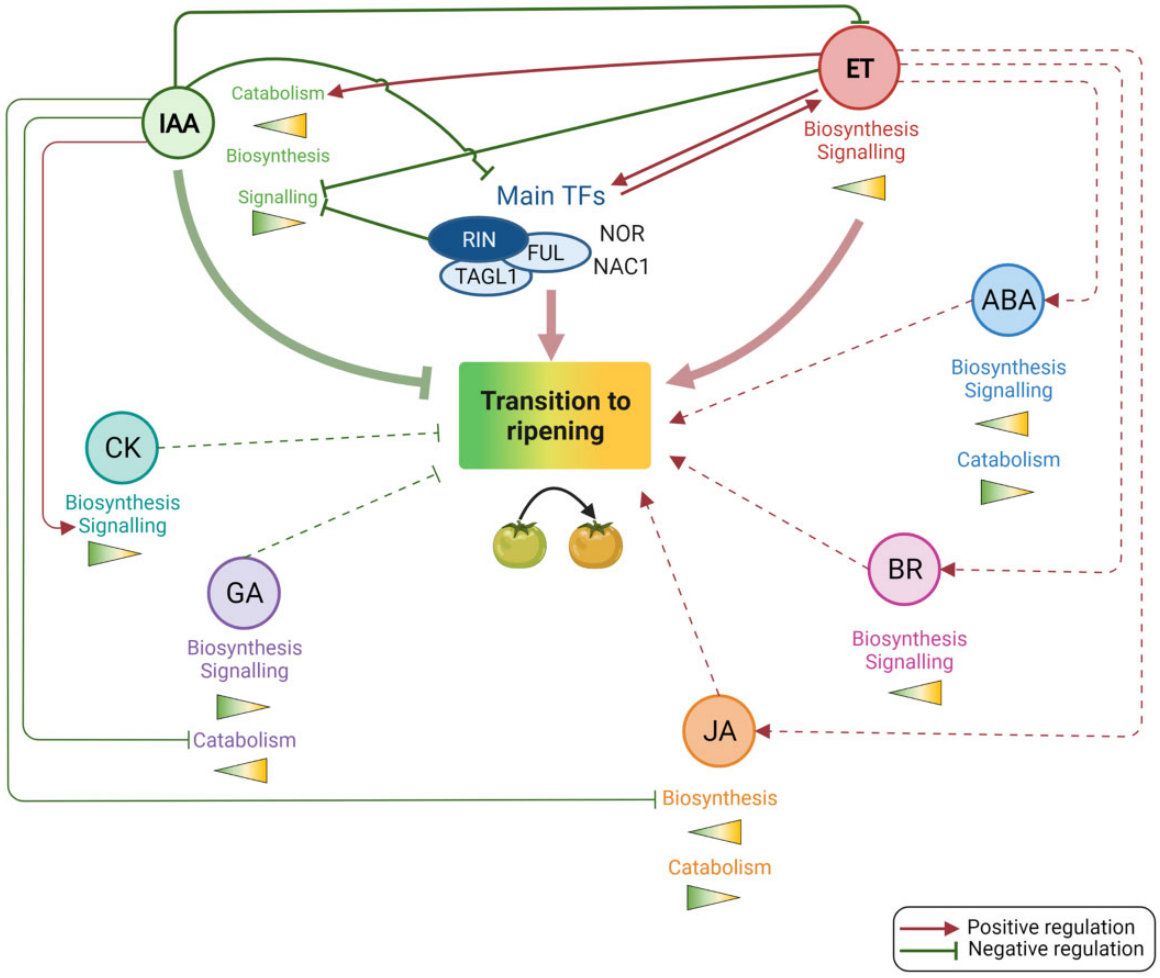

Figure 6 Multihormonal control of the transcriptomic changes associated with the onset of tomato fruit ripening. Ethylene biosynthesis and signaling increases at LMG which promotes ripening initiation in conjunction with key TFs (*RIN*, *FUL1*, *TAGL1*, *NOR*, and *NAC1*). Concomitantly, IAA concentration decreases after LMG stage via downregulation of auxin biosynthesis genes (*TAA1-like4*, *YUC-like4*, and *YUC6-like*) and IAA inactivation via upregulation of auxin conjugation/oxidation genes (*SlGH3.2*, *SlGH3.9*, and *SlDAO1*). These changes in free IAA and conjugated IAA forms are promoted by ethylene. At the ripening onset, genes encoding negative regulators of auxin signaling (*ARF2*, *ARF17*, *AUX/IAA3*, and *SlSAUR69*) are upregulated, leading to the inhibition of auxin signaling and response (Hao et al., 2015; Shin et al., 2019), while positive auxin signaling genes (*TIR1* and *ARF6A*) are downregulated. RIN has been reported to reduce auxin signaling through inducing *SlSAUR69* expression, which alters tissue distribution of auxin by blocking its transport (Shin et al., 2019). High levels of auxin hamper the onset of ripening, through downregulating key ripening regulators (*RIN*, *FUL1*, *TAGL1*, *NOR*, and *NAC1*), System-2 ethylene biosynthesis and signaling genes (*ACS2*, *ACS4*, *ACO1*, *ETR3*, *CTR1*, *AP2a*, and *ERF.E1*). Auxin also represses JA biosynthesis through inactivating their biosynthetic genes (*LOXB*, *LOXC*, and *SlJAR7*). On the other hand, auxin promotes GA signaling by blocking GA catabolism genes (*SlGA2ox2*). Also, auxin seems to promote CK by activating positive regulators of CK signaling genes (*SlPRR4*) and repressing negative regulators (*SlRR7* and *SlRR4*). Notably, consistent with their roles in promoting different aspects of ripening, BR biosynthesis and signaling genes (*SlCPD*, *SlCYP85A1*, *SlBR1*, *SlBES1*, and *SlBZR1*) and ABA biosynthesis and signaling genes (*SlSDR*, *SlMoCo*, *SlPYL1/2*, *SlSnRK2.1*, *SlSnRK2.3*, *SlSnRK2.7*, and *SlABI5-like*) are upregulated (Zhang et al., 2009; Zhu et al., 2015). Dotted arrows indicate possible regulation.

contribution of inner tissues to this process. Moreover, while so far, most transcriptomic profiling of fruit ripening has mainly focused on the changes occurring in pericarp tissues between MG and Br stages, our study addresses the changes between EMG and LMG stages, in gel and pericarp separately. The data reveal that the transition to ripening is initiated at first in locular gel before extending to pericarp. This is consistent with our recent findings that locular tissues play an essential role in controlling fruit texture and firmness (Huang et al., 2021). Our genome-wide transcriptomic analysis reveals that a wide diversity of transcription factor families are engaged in the global reprogramming of gene expression, thereby highlighting the extent of the transcriptomic changes underlying the transition to ripening. In particular, the study identified transcription factors that are specifically regulated during the MG stage in the gel but not in pericarp, thereby providing potential targets toward deciphering the initial factors and events that trigger the transition to ripening. The potential roles of these transcription factors

in the ripening program remain to be elucidated. In this regard, the outcome of our study provides an essential resource for future studies aiming to further decipher the regulation mechanisms of fruit ripening. Our data also bring evidence for a multihormonal control of the transition to ripening and show that altered auxin homeostasis disturbs the overall hormonal balance. The study reveals the antagonistic cross-talk between auxin and ethylene operating at this developmental shift. Building on the achievement of the present work, we propose a model enriched with the data that depicts the multihormonal control of the transcriptomic reprogramming leading to the transition from System-1 to System-2 of ethylene production at the onset of climacteric ripening (Figure 6).

Materials and methods

Plant material and sampling

Tomato (*Solanum lycopersicum L.* cv Micro-Tom) plants were grown under standard culture chamber conditions (14 h: 10 h, 25°C: 20°C, light: dark cycle, respectively, 80% relative humidity, 250 mol m^{-2} s^{-1} intense light). The flowers were tagged at the anthesis stage and fruits were sampled at different stages. For hormonal profiling and transcriptomic analysis in normal ripening conditions 10 fruits from 6 different plants per replicate were collected at EMG (33-day post anthesis [DPA]), LMG (36 DPA), Breaker (Br), and Br + 4 days. We sampled tomato at different DPAs around the MG stage, which allowed defining two categories differing by their ability to reach full ripening with a few days lag. In this way, we were able to define fruits corresponding to 33 DPA as EMG because 90% of them reach the full ripening stage 2–4 days later than LMG (36 DPA) of which 99% were able to fully ripe. Then gel (without seeds) and pericarp were separated and samples were frozen in liquid nitrogen, immediately after separation and stored at −80°C. Three independent biological replicates were performed for each experiment.

Hormonal profiling

Frozen fruit samples were ground with Tissue Lyser II (Qiagen, France) by applying two cycles of 45 s at 300 Hz. A total of 300 mg of ground tissue was extracted with 700 µL of pre-cooled (−20°C) extraction methyl tert-butyl ether/methanol (75/5, v/v) solvent. After mixing by vortexing, samples were sonicated for 3 min in an ultrasonic bath. A volume of 700 µL of pre-cooled water/methanol (75/25, v/v) solution was added and the samples were again thoroughly vortexed for 30 s and sonicated for 3 min. The samples were centrifuged at 14,000 rpm for 3 min at 5°C. Around 500 µL of the hydrophilic phase was transferred to a fresh 1.5-mL microcentrifuge tube and dried down using a SpeedVac concentrator at 35°C. The dried pellets were resuspended in acetonitrile/water (20/80, v/v) solution with a final concentration of 10 $mg{\cdot}mL^{-1}$. Analysis was performed by ultrahigh-performance liquid chromatography-multiple reaction monitoring (U-HPLC-MRM). U-HPLC system (Dionex Ultimate 3000, Thermo Scientific) was equipped with a Hypersil Gold AQ (100 × 2.1 mm, 1.9 µm Thermo Scientific) heated at 45°C. Five microliter of samples were injected. Separation was performed at a constant flow rate of 0.3 $mL{\cdot}min^{-1}$, in a gradient of solvents A (water + 0.05% v/v formic acid) and B (acetonitrile + 0.05% v/v formic acid): 1 min 5% v/v B; 8 min 5% to 96% v/v B; 1 min 96% v/v B, and re-equilibration to the initial conditions in 4 min. Mass spectrometer analysis was performed with a Qtrap 5500 mass spectrometer (AB Sciex) with electrospray ionization and MRM mode, as described by Pons et al. (2020). Phytohormones quantification was performed using Sciex OS software, concentration of standards is listed in Supplemental Table S3.

Auxin treatment

The IAA solutions were prepared at 100 µM in Milli-Q water at pH 5.6 and injected into fruits harvested at 33DPA (Su et al., 2015; Tobaruela et al., 2021). Fruits from the mock groups were injected with Milli-Q water alone. Injections have been performed using 40 µL of auxin or mock solution in the two opposite parts of fruits. Two successive treatments with exogenous auxin 24 h apart have been performed, the first at 33 DPA (EMG) and the second at 34 DPA. Tissues have been sampled for analysis 0 h, 6 h after the first treatment, and 24 h or 72 h after the second treatment (Figure 3A). Each condition includes 10 fruits collected from six different plants. Three independent biological repeats were performed for each experiment.

Ethylene and propylene treatment

Auxin and mock-treated tomato fruits 72 h after the second treatment (37 DPA), before any color change, were placed in an air-tight 22 L acrylic cabinet (Nalgene) with 10-ppm ethylene or 1,000-ppm propylene. The treatment was conducted continually; the gas environments (air, ethylene, and, propylene) were replenished every 24 h for 3 days, with at least three biological replicates for each treatment.

Ethylene production measurement

Five fruits treated with auxin, mock, auxin plus propylene, and mock plus propylene-treated fruits were placed in 120-mL jars 24 h after the second treatment (35 DPA). Jars were sealed and incubated at room temperature for 1 h, and 1 mL of headspace gas was injected into an Agilent 7820A gas chromatograph equipped with a flame ionization detector (Agilent, Santa Clara, CA, USA). Samples were compared with a reagent-grade ethylene standard of 4 ppm concentration and normalized for fruit weight. Three independent biological replicates were performed for each experiment.

RNA extraction

Fruit samples stored at −80°C were homogenized to powder with the ball grinder Tissue Lyser II (Qiagen, France) by applying two cycles of 45 s at 300 Hz. Total RNA from gel and

pericarp of ten individual fruits at each developmental stage was extracted, using 200 mg of fruit powder, with ReliaPrep RNA Tissue Miniprep System kit (Promega, France, Ref. Z6112) according to the manufacturer's instructions. The total RNA sample was then treated with DNA-free DNA Removal Kit (Invitrogen, France) to remove DNA. The quantity and quality of RNA were assessed by measuring the optical density (OD) at 260 nm and 280 nm by a spectrophotometer (NanoDrop 330, Thermo Fisher Scientific) and 2% (w/v) gel electrophoresis.

RNA-Seq analyses

For each condition, three biological replicates were prepared. RNA quality was checked on an Agilent 2100 Bioanalyzer System, using the RNA 6000 Nano kit protocol (Agilent Technologies, Germany). RNA samples with RNA Integrity Number values of >7.5 were sent to Novogene Bioinformatics Technology Co., Ltd (Beijing, China) for cDNA library construction and sequencing on Illumina NovaSeq 6000 platform (Illumina, San Diego, CA, USA). Raw sequence corresponding to paired-end reads (2×150 bp) were treated as described by Althiab-Almasaud et al. (2021) and aligned to SLYMIC v.1.0 assembly and annotation of the *S. lycopersicum cv*. MicroTom reference genome (BioProject: PRJNA553986). The quality of alignments is listed in Supplemental Table S4.

DE and downstream analyses

DE analysis was performed with R software version 4.1.1 (https://www.r-project.org/) using the DESeq2 package version 1.30.1 with the default relative log expression (RLE) normalization method, encompassing biases caused by library size and relative size of transcriptomes (Maza et al., 2013; Love et al., 2014). The false discovery rate (FDR) was controlled by the Benjamini–Hochberg method. Genes were declared as DEGs with an adjusted $P_{(padj)} < 0.05$ using a multifactor design, then a likelihood ratio test was performed to determine if the increased likelihood of the data use in the full model is more than expected, which included the paired sample stage or treatment. The RLE normalization by DESeq2 considers that all the transcripts have the same length and does not normalize counts by transcript length. Thus, we extracted such normalized data and normalize it by transcript lengths to be able to compare transcript expressions in downstream analyses, as profile clustering. For this purpose, we divided DESeq2 normalized expressions by transcript sizes and multiplied them by the length of a raw read, as in the TomExpress platform (https://tomexpress.gbfwebtools.fr/). These normalized expressions can then be understood as (relative) estimations of transcript numbers. Lastly, the mean value of the biological replicates was calculated giving as a result the estimated transcript number for the given condition. PCA was performed with the plotPCA function of DESeq2. All graphs were plotted with ggplot2 version 3.3.3 R package. Hierarchical clustering and heatmap for the DEGs were generated with the pheatmap version 1.0.12 R package with Pearson correlation as the distance metric and a complete linkage method.

Identification of hormone-related genes in the tomato genome

Mercator4 V3.0 tool was used to automatically annotate the SLYMIC 1.0 gene/protein model 1.1 and MapMan4 to functionally categorize the genes (Schwacke et al., 2019), annotations were manually curated. In addition, annotations from Hu et al. (2021) were recovered and the database were expanded following the same pipeline (Supplemental Table S2).

Weighted gene co-expression network analysis

Co-expression network modules were identified using normalized expression values and the WGCNA package (v1.71) in R. Genes with a low level of expression below 10 and low coefficient of variation ($CV < 0.5$) among all samples were discarded and the remaining 9,563 genes were used for the analysis. The co-expression modules were obtained using the automatic network construction function with a soft threshold (power) of 8, TOMType was "signed", networkType was "signed hybrid", minModuleSize was 30, and mergeCutHeight was 0.15. The list of genes belonging to each module is available in Supplemental Table S5.

Gene ontology analysis

Gene ontology (GO) analysis of DEGs from gel and pericarp separately was performed by PANTHER GO-slim (Mi et al., 2019). Top 20 significantly enriched GO categories were selected with FDR < 0.05.

Accession numbers

Sequence data from this article can be found in the GenBank/EMBL data libraries under accession numbers listed in Supplemental Table S6. Correspondences between SLYMIC v.1.0 (Sly nomenclature) and ITAG 2.4 (Solyc) annotation (https://solgenomics.net/organism/Solanum_lycopersicum/) are available in Supplemental Table S6. All RNA sequences are available from the Sequence Read Archive at the National Center for Biotechnology Information, under accession PRJNA808237.

Supplemental data

The following materials are available in the online version of this article.

Supplemental Figure S1. Co-expression modules generated by WGCNA.

Supplemental Figure S2. Transcriptomic kinetics of main ripening TFs.

Supplemental Figure S3. GO enrichment.

Supplemental Figure S4. Transcriptomic profile of key genes associated with hormones at the onset of ripening.

Supplemental Figure S5. Endogenous levels of different hormones at ripening initiation.

Supplemental Figure S6. Effect of exogenous auxin, ethylene, and propylene treatment on fruit ripening.

Supplemental Table S1. Solanum lycopersicum putative TF genes differentially expressed in this study.

Supplemental Table S2. Hormone-related DEGs in this study.

Supplemental Table S3. Concentration of standards used for the hormone profiling.

Supplemental Table S4. Report of the counts of reads that map to a single location and summarized at the gene level.

Supplemental Table S5. Module assignment for the 9,563 genes selected for WGCNA.

Supplemental Table S6. Accession number correspondence between Solyc, Sly, and Gene Bank.

Acknowledgments

We are grateful to L. Lemonnier and D. Saint-Martin for the cultivation of tomato plants. We are also grateful to G. Marti for the metabolomic data processing and to A. Perez for the liquid chromatography mass spectrometry (LCMS) data acquisition.

Funding

This work was supported by the European Union grant H2020 TomGEM 679796, the COST Action CA18210 RoxyCOST (European Cooperation in Science and Technology, "Oxygen sensing a novel mean for biology and technology of fruit quality"), the Labex TULIP ANR-10-LABX-41 (Laboratoire d'Excellence TULIP), the FRAIB (FR3450, Fédération de Recherche Agrobiosciences, Interactions et Biodiversité), and the Vitifungen project (Fondation Jean Poupelain).

Conflict of interest statement. The authors declare no conflict of interest.

References

Althiab-Almasaud R, Chen Y, Maza E, Djari A, Frasse P, Mollet J-C, Mazars C, Jamet E, Chervin C (2021) Ethylene signaling modulates tomato pollen tube growth through modifications of cell wall remodeling and calcium gradient. Plant J **107**: 893–908

Barry CS, Llop-Tous MI, Grierson D (2000) The regulation of 1-aminocyclopropane-1-carboxylic acid synthase gene expression during the transition from System-1 to System-2 ethylene synthesis in tomato. Plant Physiol **123**: 979–986

Bemer M, Karlova R, Ballester AR, Tikunov YM, Bovy AG, Wolters-Arts M, Rossetto P de B, Angenent GC, de Maagd RA (2012) The tomato FRUITFULL homologs TDR4/FUL1 and MBP7/FUL2 regulate ethylene-independent aspects of fruit ripening. Plant Cell **24**: 4437

Böttcher C, Boss PK, Davies C (2011) Acyl substrate preferences of an IAA-amido synthetase account for variations in grape (Vitis vinifera L.) berry ripening caused by different auxinic compounds indicating the importance of auxin conjugation in plant development. J Exp Bot **62**: 4267–4280

Brecht J (1987) Locular gel formation in developing tomato fruit and the initiation of ethylene production. HortScience **22**: 476–479

Chernys JT, Zeevaart JAD (2000) Characterization of the 9-cis-epoxycarotenoid dioxygenase gene family and the regulation of abscisic acid biosynthesis in avocado. Plant Physiol **124**: 343–354

Chung MY, Vrebalov J, Alba R, Lee J, McQuinn R, Chung JD, Klein P, Giovannoni J (2010) A tomato (Solanum lycopersicum) APETALA2/ERF gene, SlAP2a, is a negative regulator of fruit ripening. Plant J **64**: 936–947

Davey JE, Van Staden J (1978) Endogenous cytokinins in the fruits of ripening and non-ripening tomatoes. Plant Sci Lett **11**: 359–364

Diretto G, Frusciante S, Fabbri C, Schauer N, Busta L, Wang Z, Matas AJ, Fiore A, Rose JKC, Fernie AR, et al. (2020) Manipulation of β-carotene levels in tomato fruits results in increased ABA content and extended shelf life. Plant Biotechnol J **18**: 1185–1199

Dostal HC, Leopold AC (1967) Gibberellin delays ripening of tomatoes. Science **158**: 1579–1580

Fujisawa M, Nakano T, Ito Y (2011) Identification of potential target genes for the tomato fruit-ripening regulator RIN by chromatin immunoprecipitation. BMC Plant Biol **11**: 26

Fujisawa M, Shima Y, Nakagawa H, Kitagawa M, Kimbara J, Nakano T, Kasumi T, Ito Y (2014) Transcriptional regulation of fruit ripening by tomato FRUITFULL homologs and associated MADS box proteins. Plant Cell **26**: 89

Gao Y, Wei W, Zhao X, Tan X, Fan Z, Zhang Y, Jing Y, Meng L, Zhu B, Zhu H, et al. (2018) A NAC transcription factor, NOR-like1, is a new positive regulator of tomato fruit ripening. Hortic Res **5**: 75

Giovannoni J, Nguyen C, Ampofo B, Zhong S, Fei Z (2017) The epigenome and transcriptional dynamics of fruit ripening. Annu Rev Plant Biol **68**: 61–84

Grierson D (2014) Ethylene biosynthesis. Fruit Ripening: Physiology, Signalling and Genomics 178–192

Hao Y, Hu G, Breitel D, Liu M, Mila I, Frasse P, Fu Y, Aharoni A, Bouzayen M, Zouine M (2015) Auxin response factor SlARF2 is an essential component of the regulatory mechanism controlling fruit ripening in tomato. PLoS Genet **11**: e1005649

Hayashi K-I, Arai K, Aoi Y, Tanaka Y, Hira H, Guo R, Hu Y, Ge C, Zhao Y, Kasahara H, et al. (2021) The main oxidative inactivation pathway of the plant hormone auxin. Nat Commun **12**: 1–11

Hu G, Huang B, Wang K, Frasse P, Maza E, Djari A, Benhamed M, Gallusci P, Li Z, Zouine M, et al. (2021) Histone posttranslational modifications rather than DNA methylation underlie gene reprogramming in pollination-dependent and pollination-independent fruit set in tomato. New Phytol **229**: 902–919

Hu S, Liu L, Li S, Shao Z, Meng F, Liu H, Duan W, Liang D, Zhu C, Xu T, et al. (2020) Regulation of fruit ripening by the brassinosteroid biosynthetic gene SlCYP90B3 via an ethylene-dependent pathway in tomato. Hortic Res **7**: 1–13

Huang B, Hu G, Wang K, Frasse P, Maza E, Djari A, Deng W, Pirrello J, Burlat V, Pons C, et al. (2021) Interaction of two MADS-box genes leads to growth phenotype divergence of all-flesh type of tomatoes. Nat Commun **12**: 1–14

Itkin M, Seybold H, Breitel D, Rogachev I, Meir S, Aharoni A (2009) TOMATO AGAMOUS-LIKE 1 is a component of the fruit ripening regulatory network. Plant J **60**: 1081–1095

Ito Y, Nishizawa-Yokoi A, Endo M, Mikami M, Shima Y, Nakamura N, Kotake-Nara E, Kawasaki S, Toki S (2017) Re-evaluation of the rin mutation and the role of RIN in the induction of tomato ripening. Nat Plants **3**: 866–874

Jiang Y, Joyce DC, Macnish AJ (2014) Effect of abscisic acid on banana fruit ripening in relation to the role of ethylene. J Plant Growth Regul **19**: 106–111

Karlova R, Rosin FM, Busscher-Lange J, Parapunova V, Do PT, Fernie AR, Fraser PD, Baxter C, Angenent GC, de Maagd RA (2011) Transcriptome and metabolite profiling show that APETALA2a is a major regulator of tomato fruit ripening. Plant Cell **23**: 923–941

Klee HJ, Giovannoni JJ (2011) Genetics and control of tomato fruit ripening and quality attributes. Annu Rev Genet **45**: 41–59

Kou X, Zhao Y, Wu C, Jiang B, Zhang Z, Rathbun JR, He Y, Xue Z (2018) SNAC4 and SNAC9 transcription factors show contrasting

effects on tomato carotenoids biosynthesis and softening. Postharvest Biol Technol **144**: 9–19

Kumar R, Tamboli V, Sharma R, Sreelakshmi Y (2018) NAC-NOR mutations in tomato Penjar accessions attenuate multiple metabolic processes and prolong the fruit shelf life. Food Chem **259**: 234–244

Lelièvre J-M, Latchè A, Jones B, Bouzayen M, Pech J-C (1997) Ethylene and fruit ripening. Physiol Plant **101**: 727–739

Li J, Tao X, Bu J, Ying T, Mao L, Luo Z (2017) Global transcriptome profiling analysis of ethylene-auxin interaction during tomato fruit ripening. Postharvest Biol Technol **130**: 28–38

Li J, Tao X, Li L, Mao L, Luo Z, Khan ZU, Ying T (2016) Comprehensive RNA-seq analysis on the regulation of tomato ripening by exogenous auxin. PLoS One **11**: e0156453

Li S, Chen K, Grierson D (2021) Molecular and hormonal mechanisms regulating fleshy fruit ripening. Cells **10**: 1136

Li S, Zhu B, Pirrello J, Xu C, Zhang B, Bouzayen M, Chen K, Grierson D (2020) Roles of RIN and ethylene in tomato fruit ripening and ripening-associated traits. New Phytol **226**: 460–475

Liu M, Chen Y, Chen Y, Shin J-H, Mila I, Audran C, Zouine M, Pirrello J, Bouzayen M (2018) The tomato Ethylene Response Factor Sl-ERF.B3 integrates ethylene and auxin signaling via direct regulation of *Sl-Aux/IAA27*. New Phytol **219**: 631–640

Liu M, Pirrello J, Chervin C, Roustan J-P, Bouzayen M (2015) Ethylene control of fruit ripening: revisiting the complex network of transcriptional regulation. Plant Physiol **169**: 2380–2390

Liu Y, Shi Y, Su D, Lu W, Li Z (2021) SlGRAS4 accelerates fruit ripening by regulating ethylene biosynthesis genes and SlMADS1 in tomato. Hortic Res **8**: 3

Love MI, Huber W, Anders S (2014) Moderated estimation of fold change and dispersion for RNA-seq data with DESeq2. Genome Biol **15**: 1–21

Maza E, Frasse P, Senin P, Bouzayen M, Zouine M (2013) Comparison of normalization methods for differential gene expression analysis in RNA-Seq experiments. Commun Integr Biol **6**: e25849

McMurchie EJ, McGlasson WB, Eaks IL (1972) Treatment of fruit with propylene gives information about the biogenesis of ethylene. Nature **237**: 235–236

Mi H, Muruganujan A, Ebert D, Huang X, Thomas PD (2019) PANTHER version 14: more genomes, a new PANTHER GO-slim and improvements in enrichment analysis tools. Nucleic Acids Res **47**: D419–D426

Nakatsuka A, Murachi S, Okunishi H, Shiomi S, Nakano R, Kubo Y, Inaba A (1998) Differential expression and internal feedback regulation of 1-aminocyclopropane-1-carboxylate synthase, 1-aminocyclopropane-1-carboxylate oxidase, and ethylene receptor genes in tomato fruit during development and ripening. Plant Physiol **118**: 1295–1305

Oeller PW, Lu M-WW, Taylor LP, Pike DA, Theologis AA (1991) Reversible inhibition of tomato fruit senescence by antisense RNA. Science **254**: 437–439

Pirrello J, Prasad BN, Zhang W, Chen K, Mila I, Zouine M, Latché A, Pech JC, Ohme-Takagi M, Regad F, et al. (2012) Functional analysis and binding affinity of tomato ethylene response factors provide insight on the molecular bases of plant differential responses to ethylene. BMC Plant Biol **12**: 190

Van de Poel B, Vandenzavel N, Smet C, Nicolay T, Bulens I, Mellidou I, Vandoninck S, Hertog ML, Derua R, Spaepen S, et al. (2014) Tissue specific analysis reveals a differential organization and regulation of both ethylene biosynthesis and E8 during climacteric ripening of tomato. BMC Plant Biol **14**: 11

Pons S, Fournier S, Chervin C, Bécard G, Rochange S, Dit Frey NF Pagès, VP (2020) Phytohormone production by the arbuscular mycorrhizal fungus Rhizophagus irregularis. PLoS One **15**: e0240886

Schwacke R, Ponce-Soto GY, Krause K, Bolger AM, Arsova B, Hallab A, Gruden K, Stitt M, Bolger ME, Usadel B (2019) MapMan4: a refined protein classification and annotation framework applicable to multi-omics data analysis. Mol Plant **12**: 879–892

Shen J, Tieman D, Jones JB, Taylor MG, Schmelz E, Huffaker A, Bies D, Chen K, Klee HJ (2014) A 13-lipoxygenase, TomloxC, is essential for synthesis of C5 flavour volatiles in tomato. J Exp Bot **65**: 419–428

Shin JH, Mila I, Liu M, Rodrigues MA, Vernoux T, Pirrello J, Bouzayen M (2019) The RIN -regulated Small Auxin-Up RNA SAUR 69 is involved in the unripe-to-ripe phase transition of tomato fruit via enhancement of the sensitivity to ethylene. New Phytol **222**: 820–836

Shinozaki Y, Nicolas P, Fernandez-Pozo N, Ma Q, Evanich DJ, Shi Y, Xu Y, Zheng Y, Snyder SI, Martin LBB, et al. (2018) High-resolution spatiotemporal transcriptome mapping of tomato fruit development and ripening. Nat Commun **9**: 364

Soto A, Ruiz KB, Ravaglia D, Costa G, Torrigiani P (2013) ABA may promote or delay peach fruit ripening through modulation of ripening- and hormone-related gene expression depending on the developmental stage. Plant Physiol Biochem **64**: 11–24

Sravankumar T, Akash, Naik NK, Kumar R (2018) A ripening-induced SlGH3-2 gene regulates fruit ripening via adjusting auxin-ethylene levels in tomato (Solanum lycopersicum L.). Plant Mol Biol **98**: 455–469

Su L, Diretto G, Purgatto E, Danoun S, Zouine M, Li Z, Roustan JP, Bouzayen M, Giuliano G, Chervin C (2015) Carotenoid accumulation during tomato fruit ripening is modulated by the auxin-ethylene balance. BMC Plant Biol **15**: 114

Tao X, Wu Q, Li J, Wang D, Nassarawa SS, Ying T (2021) Ethylene biosynthesis and signal transduction are enhanced during accelerated ripening of postharvest tomato treated with exogenous methyl jasmonate. Sci Hortic (Amsterdam) **281**: 109965

Tobaruela EdC, Gomes BL, Bonato VC de B, de Lima ES, Freschi L, Purgatto E (2021) Ethylene and auxin: hormonal regulation of volatile compound production during tomato (Solanum lycopersicum L.) (fruit ripening. Front Plant Sci **12**: 2724

Wang R, Tavano EC da R, Lammers M, Martinelli AP, Angenent GC, de Maagd RA (2019) Re-evaluation of transcription factor function in tomato fruit development and ripening with CRISPR/Cas9-mutagenesis. Sci Rep **9**: 1–10

Zhang L, Kang J, Xie Q, Gong J, Shen H, Chen Y, Chen G, Hu Z (2020) The basic helix-loop-helix transcription factor bHLH95 affects fruit ripening and multiple metabolisms in tomato. J Exp Bot **71**: 6311–6327

Zhang M, Yuan B, Leng P (2009) The role of ABA in triggering ethylene biosynthesis and ripening of tomato fruit. J Exp Bot **60**: 1579–1588

Zhu T, Tan WR, Deng XG, Zheng T, Zhang DW, Lin HH (2015) Effects of brassinosteroids on quality attributes and ethylene synthesis in postharvest tomato fruit. Postharvest Biol Technol **100**: 196–204